A Possible Autoimmune Parathyroiditis Following Ozone Inhalation

II. A Histopathologic, Ultrastructural, and Immunofluorescent Study

O. S. Atwal, BVSc, PhD, B. S. Samagh, DVM, PhD, and M. K. Bhatnagar, BVSc, PhD

Histologic, ultrastructural, and immunofluorescent changes in the parathyroid glands of rabbits have been studied after 48 hours of ozone inhalation at a dosage of 0.75 ppm. The frequent changes observed included hyperplastic parathyroiditis followed by capillary proliferation and leukocytic infiltration. The progressive cytologic events consisted of the presence of eosinophilic leukocytes, reticuloendothelial and lymphocytic infiltration, disaggregation of the parenchyma, and interstitial edema. The ultrastructural changes consisted of degeneration of nuclei, atrophy of the mitochondria, dilatation and atrophy of the endoplasmic reticulum of the chief cells of the parathyroid gland, proliferation of the venous limb of the capillary network, and the prominent interstitial elements. The immunofluorescent techniques revealed positive immunologic response. These data suggest that ozone inhalation perhaps triggers an immune reaction which causes inflammatory injury to the parathyroid gland. The possibility that the modified functional chemical groups of the parathyroid gland act as autoantigen is discussed. (Am J Pathol 79:53-68, 1975)

In an earlier study,[1] morphologic evidence is presented that inhalation of a single dose of 0.75 ppm of ozone for 4 to 8 hours profoundly influenced the parathyroid gland of the rabbit. Light and electron microscope examination of parathyroid glands within 6 to 24 hours after treatment showed morphologic equivalents of hyperactivity. The hyperactive phase was observed as late as 24 to 30 hours after treatment, and the cells assumed their original ultrastructural disposition by 66 hours.

These observations suggest that cellular changes and ultrastructural cell biologic alterations of the chief cells of parathyroid gland were, perhaps, the manifestation of a specific reaction of parathyroid tissue to ozone inhalation, since no other endocrine gland revealed any change under similar morphologic scrutiny.

Several experiments in rabbits have shown that ozone inhalation results in characteristically modified proteins by further hydroxylation of tyrosine components.[2,3] These proteins act as autoantigen and show cross reactivity with heat-aggregated ovalbumin. Alteration of protein structure is sufficient to cause the formation of antibodies when ozonized protein is injected into the rabbits.

It is assumed, by analogy with the reactivity of ozone with SH groups and its special affinity for basic amino acids, that the reaction of ozone with critical residues of tyrosine and tryptophane of the PTH molecule will change the biologic and immunologic properties of the molecule. Therefore, one can postulate that the mechanism of ozone toxicity in the parathyroid gland is basically similar to the reported hydroxylation of proteins which act as autoantigen by showing cross reactivity with heat-aggregated ovalbumin.[2,3]

Accordingly, the present study was designed to investigate whether long-term inhalation of ozone produced irreversible changes in the parathyroid gland through an immunologically induced reaction. Evidence gained from the use of histopathologic, ultrastructural, and immunofluorescent techniques suggests that ozone inhalation triggers an autoimmune reaction which produces irreversible damage in the parathyroid gland of rabbits.

Materials and Methods

Three- to 6-month-old rabbits of both sexes weighing 1.5 to 3.0 kg were used in all experiments. Control and experimental animals were fed an identical diet for 2 weeks before exposure to ozone. The animals were matched by age and weight.

The animals were exposed to ozone at a concentration of 0.75 ppm for 48 hours in Plexiglas chambers.[1] The control rabbits were placed in a set of identical chambers which received air circulation. During inhalation, temperature was maintained at 25 C and humidity at 70%. The experiments were repeated with a total of six replicates.

Four animals were sacrificed at each of the following periods after inhalation treatment: 1 to 5 days, 7 to 10 days, 12 to 15 days, and 16 to 20 days. The parathyroid glands were dissected out and fixed in neutral buffered formaldehyde and prepared for histologic sections. These were stained with hematoxylin and eosin, periodic acid-Schiff (PAS) reagent, and modified Bodian method to demonstrate the agryophilic properties of secretory granules.

Fluorescent Antibody Technics

Parathyroid tissues from rabbits subjected to ozone inhalation and from control rabbits were stained with a fluorescent antibody method to determine the presence of parathyroid-specific autoantibodies in the serum of the ozonized rabbits.

For the direct fluorescent antibody technique, serum was collected from rabbits 14 days after 48 hours of ozone inhalation. Serum from 2 rabbits was pooled and precipitated at 33% saturation with ammonium sulfate. The precipitate was then dissolved in 0.01 M phosphate buffer, pH 7.4, containing 0.85% sodium chloride. The purification process was repeated a second time. The purified rabbit γ-globulin thus prepared was conjugated to fluorescein isothiocyanate by the method of Coons and Kaplan.[4] The labeled γ-globulin

was eluted with phosphate-buffered saline from unconjugated dye using a Sephadex G-25 column.

For indirect fluorescent antibody method, serum from rabbits was collected as described above. Fluorescein-labeled goat antirabbit globulin was obtained from Microbiological Associates (Bethesda, Md.).

Parathyroid glands from both control and ozonized rabbits were collected after sacrificing the animals and were quenched in liquid nitrogen immediately. Glands were then sectioned at an 8-μ thickness with International Cryostat model CT1. Sections on microscope slides were briefly air-dried and fixed in 95% ethanol for 30 seconds. Fixed sections were rinsed briefly in 0.1 M phosphate buffer, pH 7.8, prior to treatment with either unlabeled or labeled γ-globulin.

For the indirect technique, two drops of serum were placed on the sections, which were then incubated in moist chambers at 37 C for 30 minutes. After incubation, sections were washed five times in 0.1 M phosphate buffer, pH 7.8. These sections were then incubated in goat antirabbit fluorescein-labeled γ-globulin for 30 minutes, washed several times, and mounted in phosphate-buffered glycerol.

For direct labeling, the sections were incubated in a fluorescein-labeled γ-globulin (obtained from ozonized rabbits) preparation for 30 minutes, washed five times in 0.1 M phosphate buffer, pH 7.8, and mounted in phosphate-buffered glycerol.

Adrenal glands from both control and ozonized rabbits were stained with both direct and indirect methods to check the parathyroid specificity of autoantibodies present in the serum of ozonized rabbits.

The slides were read under an ultraviolet microscope equipped with HBO mercury light source and dark-field immersion condensor. On the same day, photomicrographs were taken with an automatic camera attachment using Kodak Tri X black and white film (ASA 400) and colored transparencies using Kodachrome II film (ASA 64).

For electron microscopy, 1-mm pieces of parathyroid gland tissue were harvested. These samples were immersed in cold 2.5% gluteraldehyde in 0.2 M phosphate buffer, pH 7.4. The tissues were fixed for 2 hours, washed in 0.1 M phosphate buffer for 2 hours, and then fixed in 1% osmium tetroxide in phosphate buffer, pH 7.4. The tissue was dehydrated and embedded in Epon 812. Sections were obtained with an ultramicrotome using a glass knife and were examined by electron microscopy. Corresponding 1-μ-thick sections were stained with toluidine blue and examined by light microscopy.

Results

Histology

Control

Histologic examination of the controls showed compact, coordinated clusters of chief cells separated by PAS-positive interstitium and blood capillaries. The clusters were formed by a mixture of regularly polyhydral cells with light and dark cytoplasm. The nuclei were round in shape, with finely granular chromatin network. An occasional nucleolus is present within each nucleus (Figures 1 and 2).

Ozone-Treated Rabbits

One to 5 days after treatment, considerable variation was observed between the response of the parathyroid to 48 hours of intermittent exposure to ozone and the response to 48 hours of continuous exposure to ozone.

The glands in the early posttreatment stage retained a compact, cluster-like arrangement, in contrast to those in later stages when parenchyma was severely distorted. The glands were enlarged and congested in appearance. The histologic examination revealed high cellular density with several cells undergoing mitosis (Figure 3). The cells appeared vacuolated, especially in the perivascular and subcapsular areas. The glandular parenchyma was interspersed with a proliferated capillary network which was surrounded by mononuclear cell cuffings. Intercellular edema was more conspicuous in the perivascular areas. Focal vasculitis was noticed along with degenerating endothelial lining and leukocytic infiltration of the walls of larger blood vessels (Figure 4).

Seven to Ten Days After Treatment

From this stage onward, the parenchyma exhibited changes similar to immune lesions. Atrophy and disaggregation of the glandular parenchyma and interstitial infiltration with eosinophilic leukocytes and mononuclear cells were the predominant changes at this stage. The proliferation of endothelium and the appearance of new capillary buds were conspicuous, as was the disruption of the capsular covering (Figure 5). The most characteristic pathologic change at this stage and subsequent stages was focal proliferation of the pericapillary connective tissue intermingling with scattered eosinophilic masses which were weakly PAS positive.

Twelve to Fifteen Days After Treatment

There was intense atrophy, and the prominent lesions were: reticuloendothelial proliferation, increased vascular permeability, variable leukocytic infiltration, and eosinophilic necrosis of the glandular chief cells (Figures 6 and 7).

Sixteen to Twenty Days After Treatment

Continued intense atrophy, total disruption of the parenchyma, and mononuclear cells infiltration were the prominent changes at this stage. The lesions showed large confluent masses of mononuclear cells replacing the disintegrating parathyroid tissue (Figures 8 and 9), loss of compact cellular pattern, and the resulting sclerosis.

Ultrastructural Changes

The changes observed immediately after treatment are termed acute, and those seen after a longer period after treatment are termed chronic. The fine structure of the parathyroid gland is similar to that already

described in an earlier study [1] (Figure 10). During the stage immediately
following the treatment (1 to 5 days), the chief cells had the characteristic
features of a high index of synthetic secretory activity, as indicated by the
prominent Golgi complexes, proliferated endoplasmic reticulum, exten-
sive dispersion of free ribosomes, vacuolization, and tumefaction of the
mitochondria and their close association with dilated endoplasmic
reticulum.[1] In later stages, the chief cells were degranulated and appeared
inactive, although a few cells contained both mature and immature types
of secretory granules. In some specimens, mitochondria were found in
large numbers (Figures 11 and 12). The cell membranes in many instances
had disappeared, giving an impression that the cells were coalescing
together. Massive proliferation of interstitial tissue was conspicuous. The
vascular stroma was quite distinctive, with frequent duplication of basal
lamina of the extensively distributed capillaries. The large bundles of col-
lagen arranged in precise parallel array were present between the capil-
laries and the parenchymal tissue. Flattened fibroblasts (Veil cells) were
usually encountered in the vicinity of the vascular capillaries. The
fibroblasts were more tapering and prominent than those normally seen in
the normal parathyroid gland. The appearance of prominent collagen
bundles and fibroblasts was a distinctive diagnostic feature of the
ozonized rabbits examined 7 to 21 days after treatment (Figures 12 and
13). The capillary network of abnormal parathyroid glands was structural-
ly hetrogeneous and consisted of continuous and fenestrated capillaries.
The fenestrated capillaries constitute about 60 to 80% of the total capil-
laries (Figures 11–13). These capillaries contained several fenestrae in
cross section and were considered to belong to venous limb of the capillary
bed. Such a distinction between the venous and arterial natures of the
capillaries was based on the frequency of fenestrae and the thickness of
the endothelial cells.[6] Endothelial cells of the capillary network contained
several subcellular organelles, indicative of a higher metabolic rate.

During the chronic stage, the chief cells showed degenerating nuclei
with irregular, ragged nuclear membranes in a cog-like pattern; atrophic
endoplasmic reticulum; absence of free ribosomes; and swollen and
vacuolized mitochondria with ruptured cristae. The number and size of
the secretory and prosecretory granules were drastically reduced. Lysomes
of primary, secondary, and tertiary (phagolysosomes) types and resulting
autophagic vacuoles were increased in number (Figure 13). The en-
dothelium of proliferated small capillary buds was surrounded by
amorphous basal lamina lacking structured fibrilar elements. In some sec-
tions the hyperplastic endothelial cells contained diffusely scattered
glycogen particles. Large lipid bodies with pleomorphic interna were pres-

ent, especially in the perinuclear area of the chief cells. The lipid inclusions were electron lucent and had distinct limiting membranes. Most of the lipid bodies had stalked lamellar membranes at their peripheries and slightly dense pleomorphic martrices scattered with numerous lead granules (Figure 11). The cells were atrophic in appearance and had reduced cytoplasmic:nuclear ratios. These cells showed vacuolated and cystically dilated endoplasmic reticulum and small Golgi complexes with fewer prosecretory granules (Figure 12). The scanty rough endoplasmic reticulum was intermingled with progressively increased profiles of smooth endoplasmic reticulum. A conspicuous cytoplasmic change in the parathyroid gland chief cells at 14 days after treatment was the dispersion of large scattered individual β-glycogen particles which at higher magnification were seen to be of uniform size.

Immunofluorescence

There was no appreciable difference between the intensity of specific fluorescence seen with the indirect technique and that seen with the direct technique. In ozone-exposed rabbits treated with serum from ozonized rabbits, specific apple-green fluorescence was localized mostly at the peripheries of the parathyroid cells (Figure 14). No specific fluorescence was observed in the sections of glands of ozone-exposed rabbits when treated with normal serum (Figure 15).

Discussion

The most significant findings in this study are the specific morphologic and immunofluorescent changes seen in the parathyroid glands of ozonized rabbits. These changes began immediately after the cessation of the inhalation treatment [1] and then evolved into the specific morphologic alterations of parathyroiditis. The inflammatory lesions contained all the characteristic components of an immunologic process: initial cellular hyperplasia, disaggregation, exudative, and invasive destruction of the otherwise densely packed clusters of chief cells and eventual mononuclear cell infiltration.

The morphologic changes that develop during the course of experimental isoimmune parathyroiditis are identical at both the light and electron microscopic levels.[6-9] A significant additional feature of the ultrastructural changes of parathyroiditis during the present investigation was the vascularity of the stroma and the proliferation of the fenestrated venous limb of the capillary bed.[10] Little mention of this vascular change is found in earlier studies describing the inflammatory components of the autoimmune parathyroiditis. It has been suggested by Casley-Smith that the

fenestrae allow large molecules to pass from the tissue to the blood.[11] One can presume that, in an autoimmune inflammatory process, large molecules will leave the capillaries and accumulate in the interstitial tissue. The higher concentration of fenestrae of the venous limb of the capillary bed presently observed is consistent with Casley-Smith's hypothesis.[11] The high density of mitochondria perhaps underlies a compensatory phenomenon that augments the respiratory effort following damage to mitochondria.[12]

From the fact that changes basically similar to those already described in isoimmune parathyroiditis did occur,[6-9] one may assume that these alterations represent an injury by an autoimmune process to the parathyroid gland. Substantial evidence to support this contention is derived from the present immunofluorescent localization of antibody against parathyroid tissue of ozonized rabbits by the direct and indirect Coons' tests. The positive reaction of sera of ozonized rabbits with some structural component of chief cells of the parathyroid gland more or less resembled the immunofluorescence of the serum of the patients with idiopathic hypoparathyroidism.[13,14] However, no clinical significance could be established, nor was a correlation of antibody titer with the inflammatory damage to the glandular tissue attempted during the present study.

In recent years, much information has accumulated establishing the role of antigen–antibody complexes, per se, as pathogenic agents capable of inducing a variety of injuries.[15] Earlier investigations have shown that a tissue antigen exists in the structure of the bovine parathyroid gland and that purified extracts of parathyroid antigen stimulate the production of specific antibodies against parathyroid hormone.[16-18]

From the present inflammatory lesions and the positive immunofluorescent reaction to the serum against the parathyroid gland, it is quite natural to infer that ozone damages the glandular parenchyma and consequently releases an antigen that triggers an autoimmune reaction. Organ-specific antigen contained in the parathyroid tissue [13,14] is probably well suited to undergo a change to act as an autoantigen. The alternate explanation could be the hydroxylation of tyrosine and methionine components of PTH [19,30] which, after ozonization, undergo chemical modification. Such a modification of the immunologic properties of proteins through hydroxylation of amino acid residues has been demonstrated by Scheel *et al* [2] and Stokinger and Coffin.[3] If these findings have any general validity, then it may well be that the functional chemical groups of the parathyroid tissue undergo modification under the influence of ozone to act as antigen. This line of interpretation is well supported if we assume

that the biologic and immunologic properties of the parathyroid hormone
are changed under the oxidizing influence of ozone. Potts *et al.*[19] have
demonstrated a marked sensitivity of the immunologic properties of the
PTH to the oxidation of tyrosine.

The preliminary data on the serum assay level of calcium and
phosphorus suggest that hypoparathyroidism may well be a sequel to the
glandular disturbance induced by ozone exposure. Whether this indeed
occurs and whether the antibodies are directed against antigen residing in
the parathyroid tissue or the parathyroid hormone itself remain to be
determined. However, the present study provides an opportunity to im-
munologists, pathologists, clinicians, and environmentalists to pursue a
somewhat different future course of study in the field of ozone toxicity. Ex-
perimental investigation of immune parathyroiditis may prove to be a
good model to fill the gap between the basic similarities of experimentally
induced immunopathologic responses and certain of the naturally occur-
ring forms of idiopathic parathyroiditis in the human population.[21]

References

1. Atwal OS, Wilson T: Parathyroid-gland changes following ozone inhalation: A
    morphologic study. Arch Environ Health 28:91–100, 1974
2. Scheel LD, Dobrogorski OJ, Mountain JT, Svirbely JL, Stokinger HE: Physiologic,
    biochemical, immunological and pathologic changes following ozone exposure. J
    Appl Physiol 14:67–80, 1959
3. Stokinger HE, Coffin DL: Biologic effects of air pollutants. Air Pollution, Second
    edition, Vol I. Edited by AC Stern. New York, Academic Press, 1968, pp 446–546
4. Coons AH, Kaplan MH: Localization of antigen in tissue cells. II. Improvement in
    a method for the detection of antigen by means of fluorescent antibody. J Exp Med
    91:1–13, 1950
5. Pudney BJ, Casley-Smith JR: Differences in the numbers of fenestrae between the
    arterial and venous ends of capillaries in adrenal cortex. Experientia 26:398–399,
    1970
6. Alterhar E: Ultrastructural pathology of parathyroid glands. Curr Top Pathol
    56:2–48, 1972
7. Lupulescu A, Petrovici A, Pop A, Heitmanek C: Electron microscopic observations
    on the parathyroid gland in experimental hypoparathyroidism. Experientia 24:62–63,
    1968
8. Lupulescu A, Pop A, Merculiev E, Neascu C, Heitmanek C: Experimental iso-
    immune-hypoparathyroidism in rats. Nature (Lond) 206:415–416, 1965
9. Jankovic BD, Isvaneski M, Popeskovic L, Mitrovic K: Experimental allergic
    thyroiditis (and parathyroiditis) in neonatally thymectomized and bursectomized
    chickens: Participation of thymus in the development of disease. Int Arch Allergy
    26:18–35, 1965
10. Munger BL, Lang CM: Spontaneous diabetes mellitus in guinea pigs: The acute
    cytopathology of the islets of Langerhans. Lab Invest 29:685–702, 1973
11. Casley-Smith JR: Endothelial fenestrae in intestinal villi: Difference between the
    arterial and venous ends of the capillaries. Microvasc Res 3:49–68, 1971

12. Mustafa GM, DeLucia AJ, York GK, Arth C, Cross CE: Ozone interaction with rodent lung. II. Effects on oxygen consumption of mitochondria. J Lab Clin Med 82:357–365, 1973

13. Blizzard RM, Chee D, Davis W: The incidence of parathyroid and other antibodies in the sera of patients with idiopathic hypoparathyroidism. Clin Exp Immunol 1:119–128, 1966

14. Irvine WJ, Scarth L: Antibody to oxyphil cells of the human parathyroid and idiopathic hypoparathyroidism. Clin Exp Immunol 4:505–510, 1969

15. Cochrane CG, Dixon FJ: Cell and tissue damage through antigen–antibody complexes. Textbook of Immunopathology, Vol I. Edited by PA Meischner, HJ Müller-Eberhard. New York, Grune and Stratton, 1969, pp 94–110

16. Blizzard RM: Idiopathic hypoparathyroidism: A probable autoimmune disease. Textbook of Immunopathology, Vol II. Edited by PA Meischner, HJ Müller-Eberhard. New York, Grune and Stratton, 1969, pp 547–550

17. Kenny FM, Holliday MA: Hypoparathyroidism, moniliasis, Addison's and Hashimato's disease. N Engl J Med 271:708–713, 1964

18. Moulias R, Goust JM, Muller-Berat CN: Hypoparathyroidism and cell mediated immunity. Lancet 1:1239, 1971

19. Potts JT, et al: Parathyroid hormone: Chemical properties and structural requirements for biological and immunological activity. Rec Prog Hormone Res 22:101–151, 1966

20. Fisher JA, Oldham SB, Sizemore GW, Arnaud CD: Calcium regulated parathyroid hormone peptidase. Proc Natl Acad Sci USA 69:2341–2345, 1972

21. Van deCasseye M, Gepts W: Primary (autoimmune?) parathyroiditis. Virchows Arch [Pathol Anat] 361:257–261, 1973

Legends for Figures

Figure 1—Parathyroid chief cells arranged in compact clusters separated by scanty inter-stitium. The round nuclei contain finely granular chromatin network and an occasional nucleolus. (Control animal, original magnification × 400)

Figure 2—Parathyroid chief cells cut at varying angles. Dark cells (*DC*) and light cells (*LC*) are easily distinguished; cells are abutting on capillaries and interstitium (*arrows*). The arrange-ment of cells is compact, with no visible intercellular clefts. (Control animal, toluidine blue, original magnification × 400)

Figure 3—Parathyroid chief cells have lost somewhat a regular, cluster-like arrangement and are undergoing mitotic division (metaphase). There is apparent more cellular density. (Three days posttreatment, H&E, original magnification × 400)

Figure 4—An inflammed blood vessel with swollen endothelium (*arrow*). Note the perivascular interstitial edema, and mononuclear cells infiltration. (Five days posttreatment, H&E, original magnification × 400)
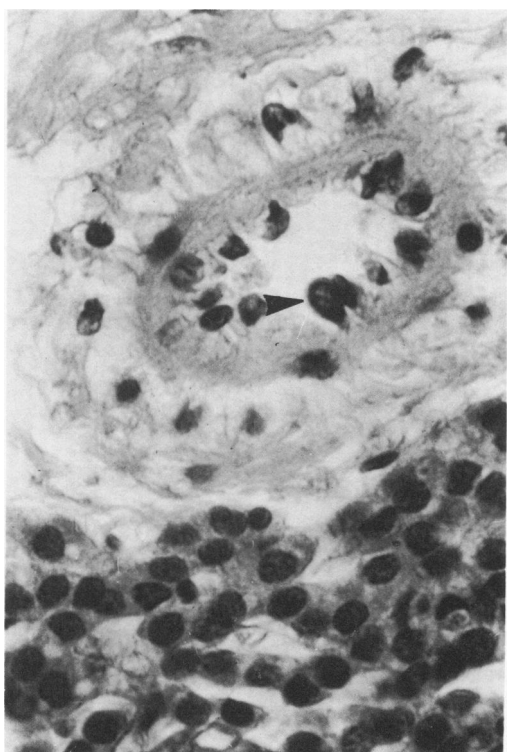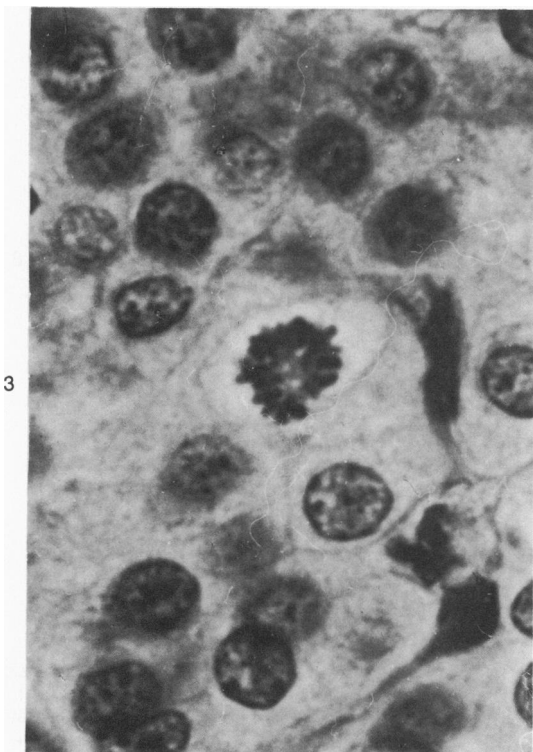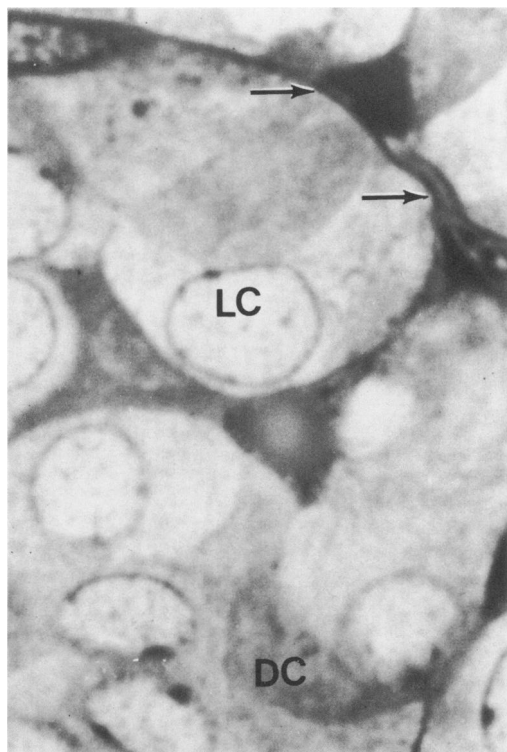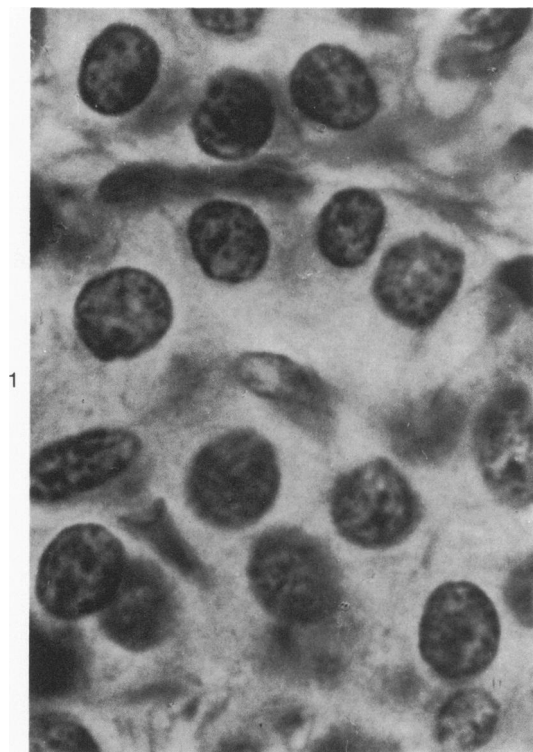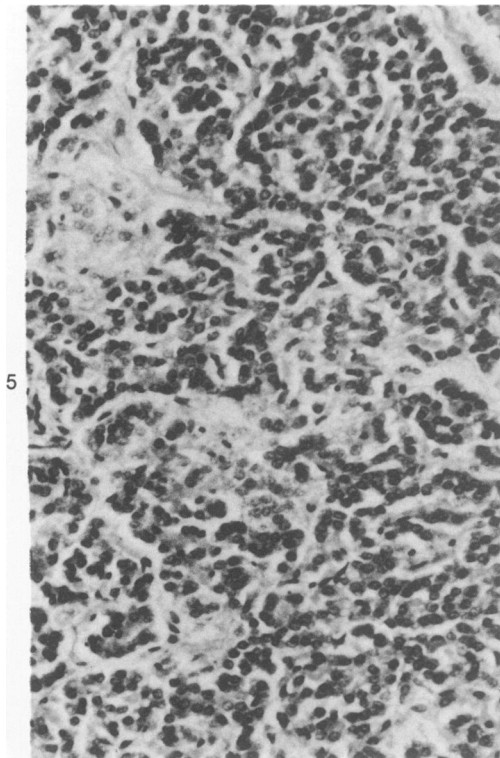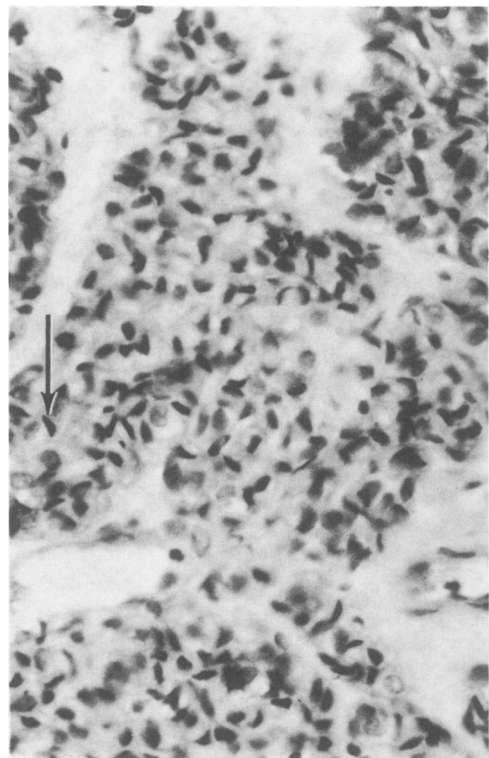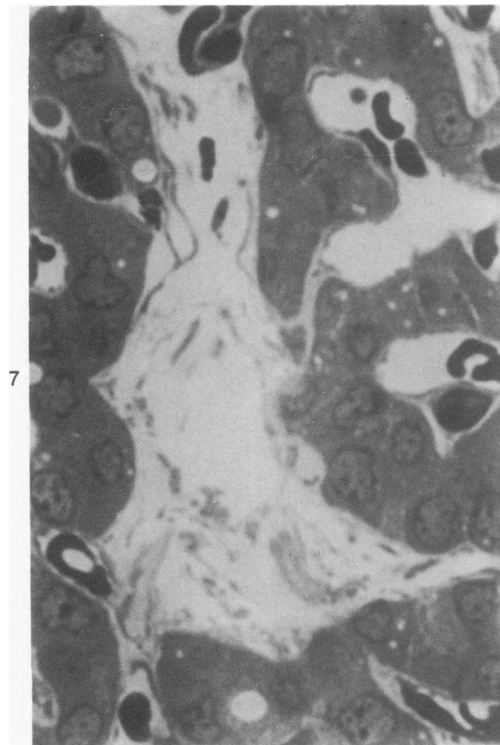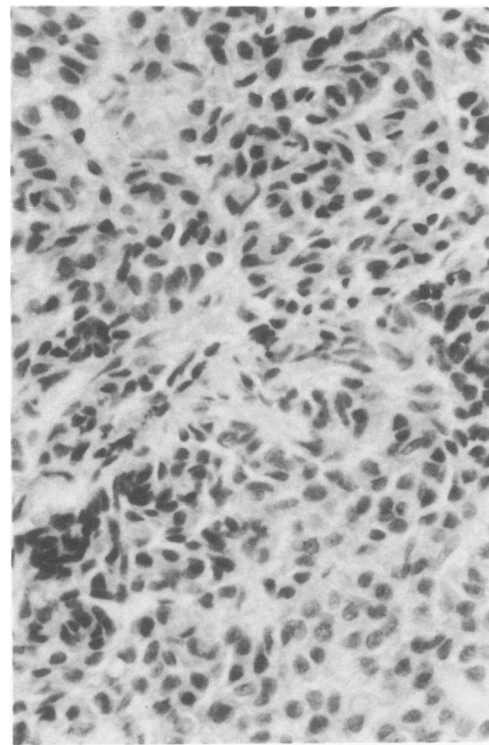
Figure 5—Disaggregated glandular parenchyma has lost its original coordinated cluster-like compact appearance. The cells have undergone atrophy, and general interstitial edema is quite apparent. (Eight days posttreatment, H&E, original magnification × 100)　　**Figure 6**—Intense atrophy of parathyroid chief cells with concurrent proliferation of reticuloendothelial cells (*arrow*). Focal areas of perivascular and interstitial edema have disrupted the parenchymal cords. (Fourteen days posttreatment, H&E, original magnification × 280)　　**Figure 7**—Cords of chief cells are dissected by highly proliferated vascular capillaries and intercellular clefts of edematous areas. The chief cells are vacuolated and contain darkly stained droplets. (Fourteen days posttreatment, toluidine blue, original magnification × 400)　　**Figure 8**—Lymphocytic infiltration and disaggregation of the parenchymal clusters of chief cells of parathyroid gland (Twenty days posttreatment, H&E, original magnification × 280).

Figure 9—A disrupted sheet of chief cells intermingled with lymphoplasmocytic cells (*arrows*); note the inflammatory edema (Twenty days posttreatment, H&E, original magnification × 400).
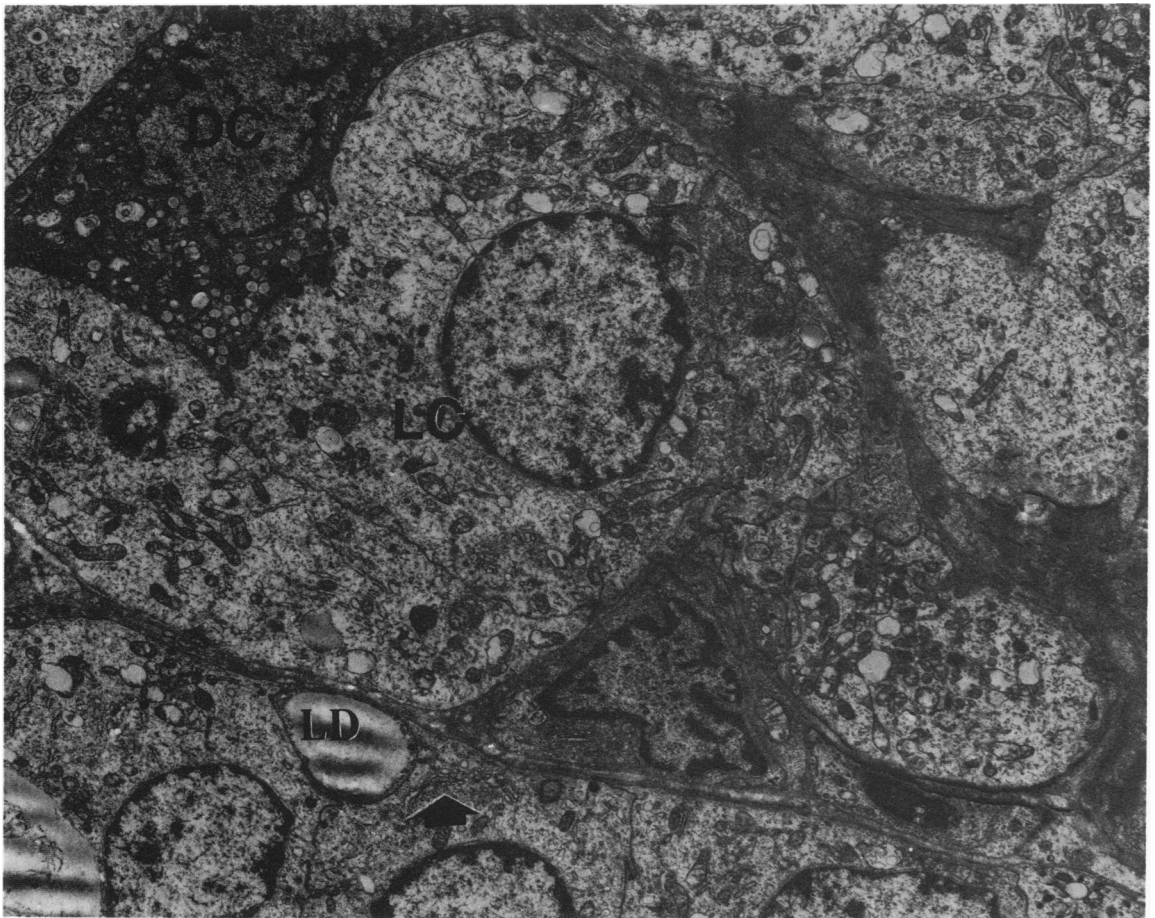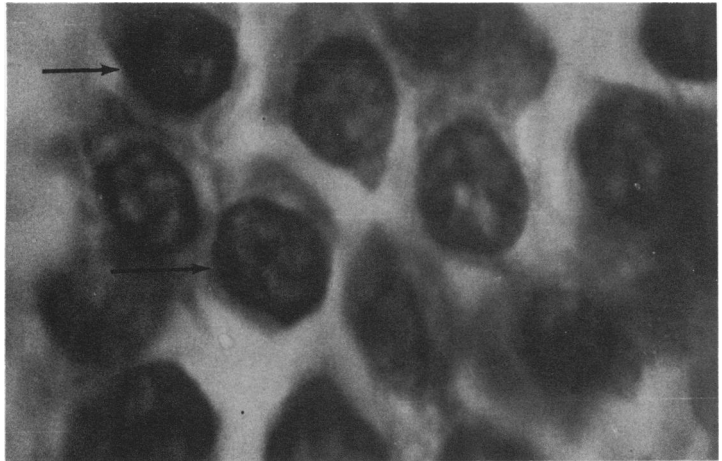
Figure 10—Several parathyroid chief cells from control rabbits showing light cells (*LC*) and dark cells (*DC*), arranged in compact clusters. The lateral cell membranes show typical infolding. Modest amount of rough endoplasmic reticulum, small Golgi complex (*large arrow*), and mitochondria are present. A few secretory granules are present in basal protion of the cytoplasm. *Ld* = lipid droplets. (Uranyl acetate and lead citrate, original magnification × 8200)
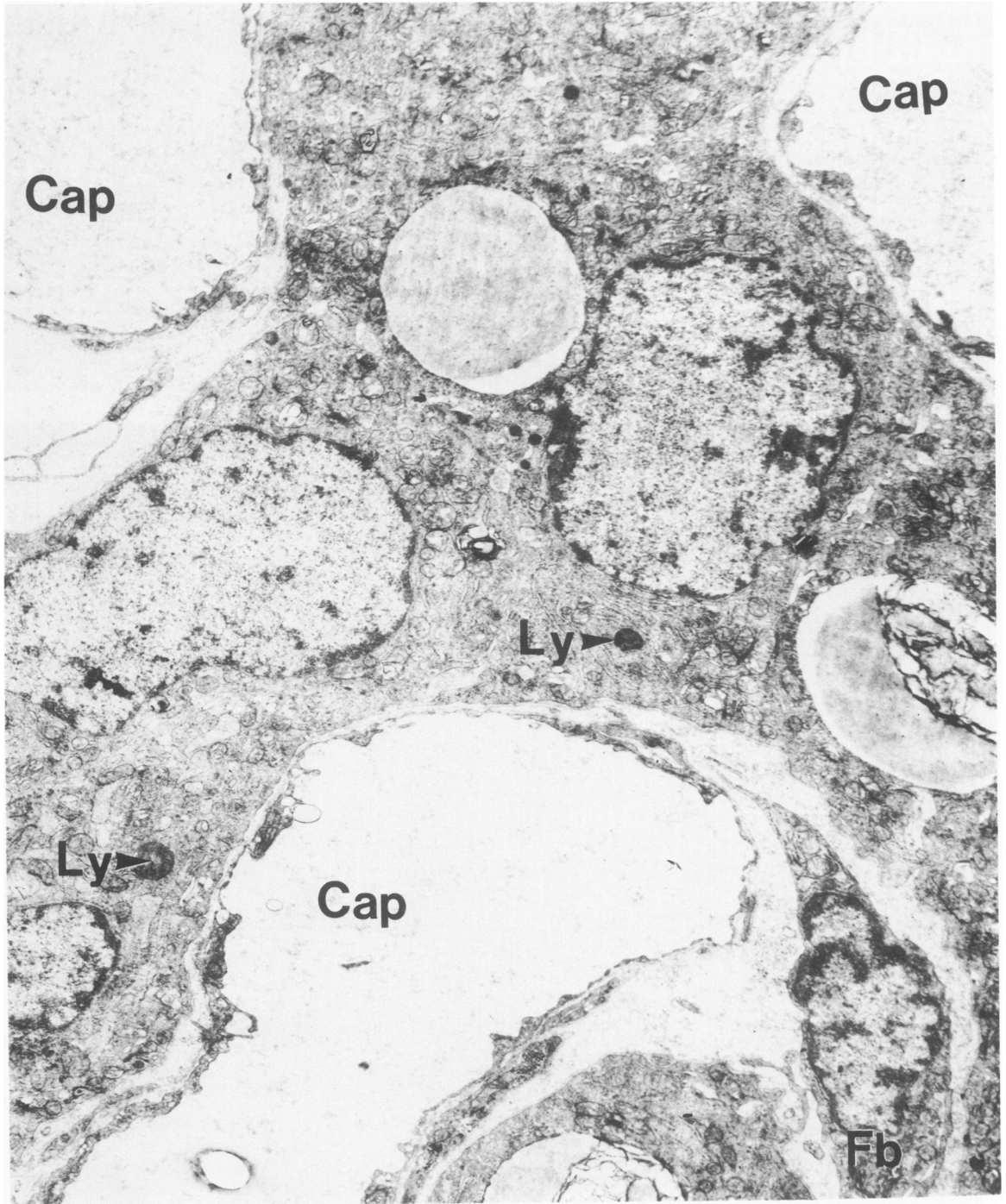
Figure 11—Several atrophic chief cells of parathyroid gland of ozone treated rabbits are dissected into single cell layer cords by overwhelming proliferated capillary sinusoids (*Cap*). Note the lipid contents of the chief cells and the atrophic mitochondria and other cell orgenelles. *Fb* = fibroblasts, *Ly* = lysosomes. (Sixteen days posttreatment, uranyl acetate and lead citrate, original magnification × 18,000)
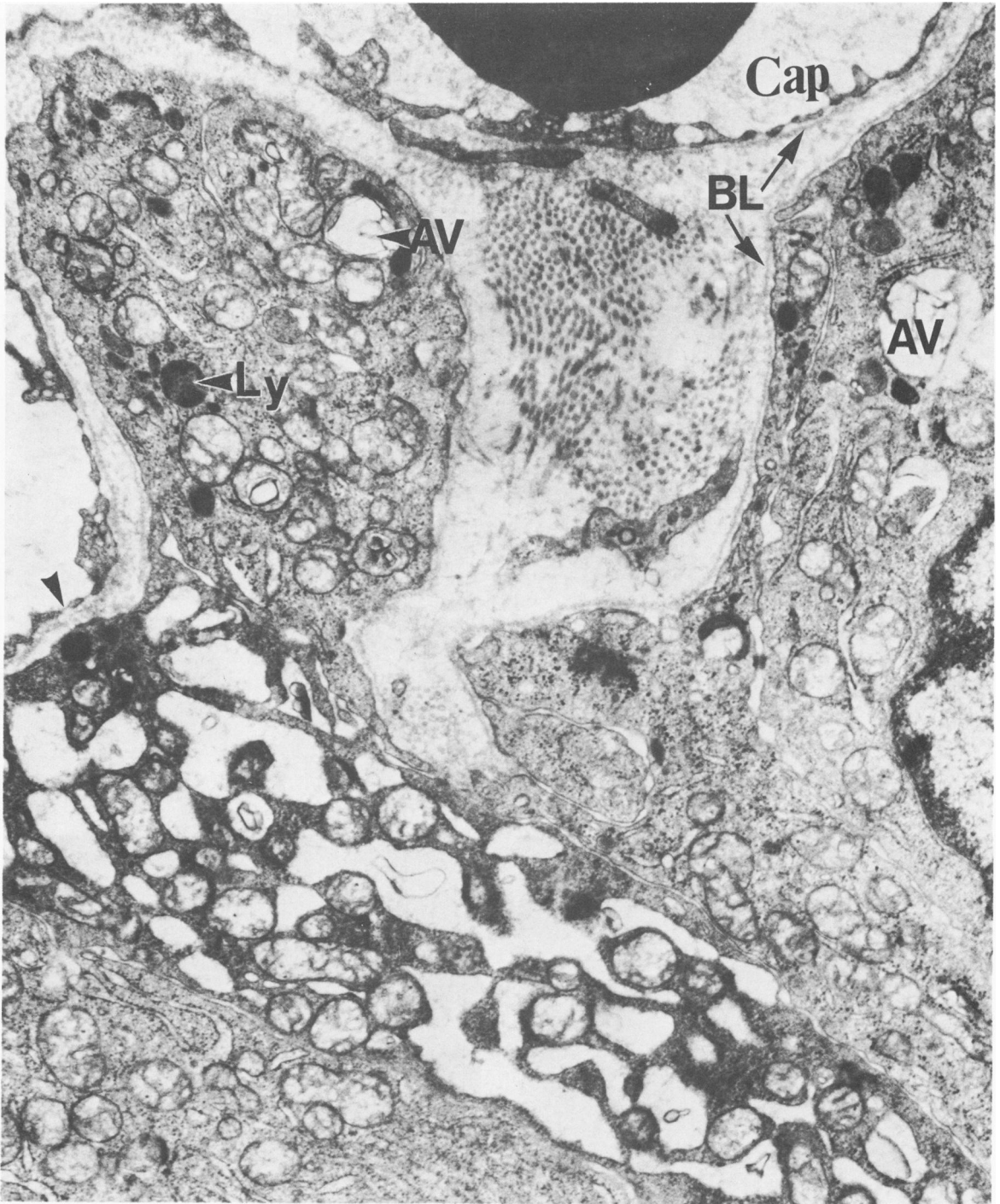
Figure 12—Portions of chief cells surrounding a capillary (*Cap*) lined with fenestrated endothelium (*arrowhead*). Note the highly dilated endoplasmic reticulum of a degenerating chief cell and the intercellular collagen separating the chief cells. *Ly* = lysosomes, *AV* = autophagic vacuoles, *BL* = basal lamina with scattered individual β-glycogen particles. (Fourteen days posttreatment, uranyl acetate and lead citrate, original magnification × 20,000)
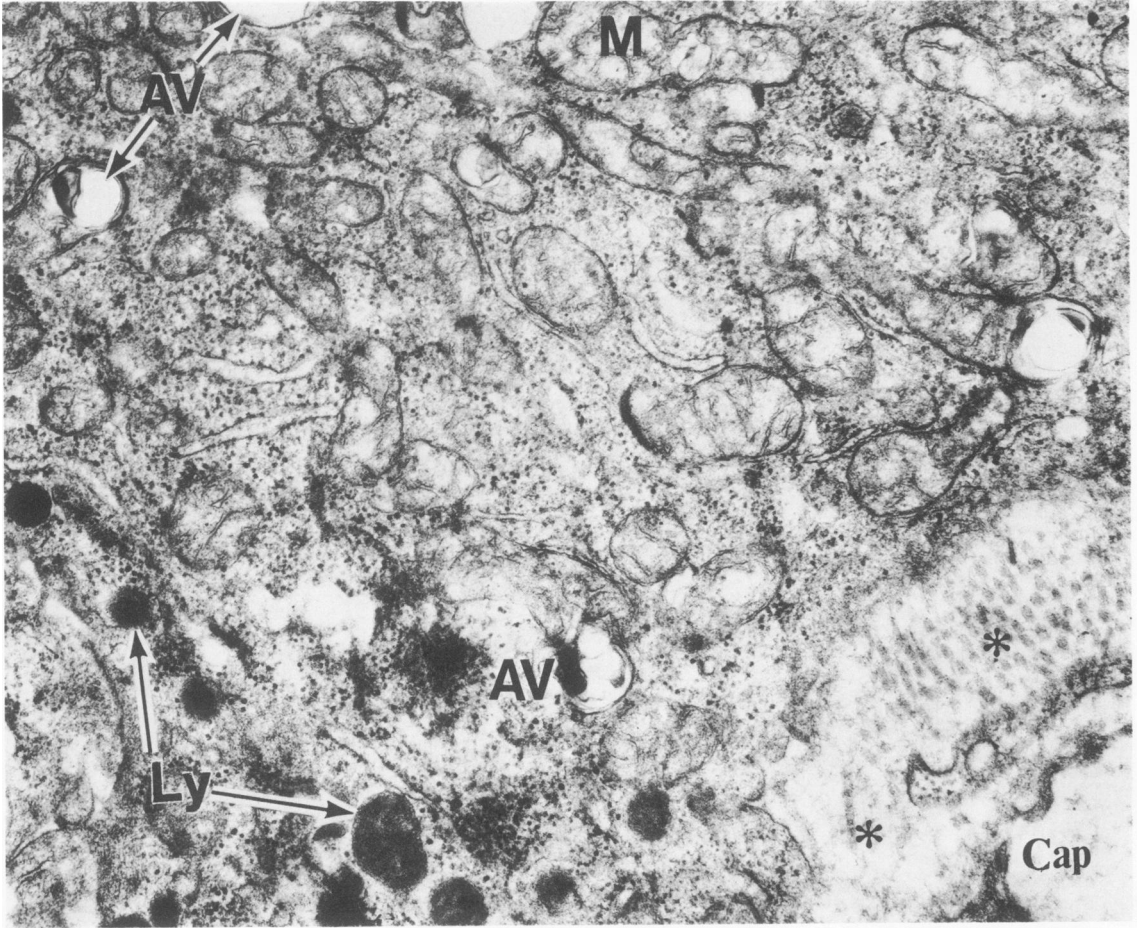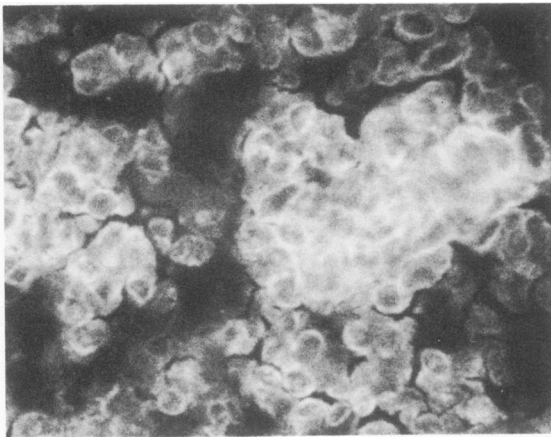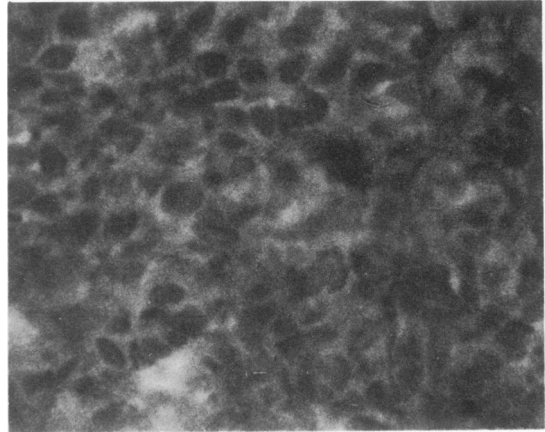
Figure 13—Portions of chief cells surrounding a fenestrated capillary (*Cap*). Note the extensive distribution of lysosomes (*Ly*) autophagic vacuoles (*AV*) and β-glycogen. Edematous connective tissue is represented by asterisks, *M* = mitochondria. (Eighteen days posttreatment uranyl acetate and lead citrate, original magnification, × 22,000)   Figure 14—Frozen sections of parathyroid gland of ozonized rabbit showing specific fluorescence primarily localized at the cell periphery (Indirect Coons test, serum from ozonized rabbits, original magnification × 280)   Figure 15—Frozen sections of parathyroid gland of ozonized rabbit showing no specific fluorescence at the cell periphery (Indirect Coons test, serum from control rabbits, original magnification × 280).